Local Field Effects in the Energy Transfer between a Chromophore and a Carbon Nanotube: A Single-Nanocompound Investigation

Cyrielle Roquelet,[†,§] Fabien Vialla,[‡] Carole Diederichs,[‡] Philippe Roussignol,[‡] Claude Delalande,[‡] Emmanuelle Deleporte,[†] Jean-Sébastien Lauret,[†] and Christophe Voisin[‡,*]

[†]Laboratoire de Photonique Quantique et Moléculaire, Institut d'Alembert, CNRS, ENS Cachan, 94235 Cachan, France and [‡]Laboratoire Pierre Aigrain, École Normale Supérieure, Université Paris Diderot, UPMC, CNRS UMR 8551, 24 Rue Lhomond, 75005 Paris, France [§]Now at Physics and Chemistry Departments, Columbia University, New York, United States

ABSTRACT

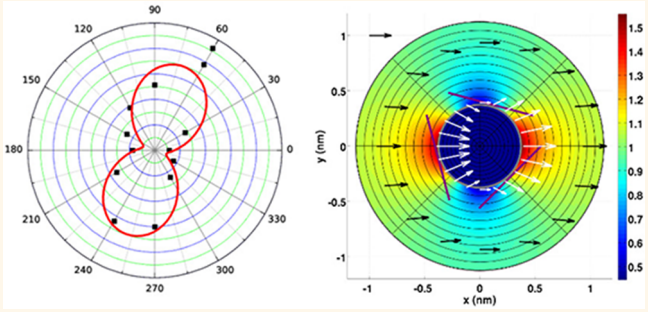

Energy transfer in noncovalently bound porphyrin/carbon nanotube compounds is investigated at the single-nanocompound scale. Excitation spectroscopy of the luminescence of the nanotube shows two resonances arising from intrinsic excitation of the nanotube and from energy transfer from the porphyrin. Polarization diagrams show that both resonances are highly anisotropic, with a preferred direction along the tube axis. The energy transfer is thus strongly anisotropic despite the almost isotropic absorption of porphyrins. We account for this result by local field effects induced by the large optical polarizability of nanotubes. We show that the local field correction extends over several nanometers outside the nanotubes and drives the overall optical response of functionalized nanotubes.

KEYWORDS: carbon nanotubes · energy transfer · photoluminescence · polarization spectroscopy · light harvesting · near field · polarizability

Single-wall carbon nanotubes (SWNTs) have attracted much attention in the last decades due to promising properties for future applications.[1] However, it appeared rapidly that their performances can be highly enhanced by means of functionalization. This allows combining the exceptional properties of nanotubes with those of various molecules.[2,3] In particular, in view of light-harvesting or opto-electronics applications, the combination of a photoactive molecule (chromophore) with nanotubes is particularly attractive.[4] Energy transfer, charge transfer, and luminescence quenching are some of the possible effects that can result from the combination of chromophores with nanotubes and could possibly lead to new opportunities in organic photovoltaics or biolabeling. In all cases, the goal is to exploit the large optical absorption of the chromophore to funnel the light energy into the device. Therefore, it is essential to know how the optical response of the chromophore is affected by the presence of the nanotube and how efficient the coupling between the chromophore and the nanotube is.

Here, we focus on noncovalently bound porphyrin/carbon nanotube compounds that display efficient energy transfer: absorption in the porphyrin molecules results in enhanced near-infrared (NIR) emission from the nanotube. We performed an all-optical investigation of the coupling between the chromophore and the nanotube at the single-nanocompound scale by means of micro-photoluminescence excitation spectroscopy and polarization spectroscopy. Each (of a few tens of specimens) nanocompound shows two resonances arising from intrinsic excitation of the nanotube and from energy transfer from the porphyrin. The weak temperature dependence of the transfer efficiency (down to 10 K) is compatible with a purely electronic process. Moreover, polarization spectroscopy allowed us to reveal original antenna effects that lead to a peculiar coupling between light and the nanocompounds. We show that the local field effects due to the large optical polarizability of the nanotubes

* Address correspondence to christophe.voisin@lpa.ens.fr.

Received for review June 11, 2012 and accepted September 17, 2012.

Published online September 24, 2012
10.1021/nn302566e

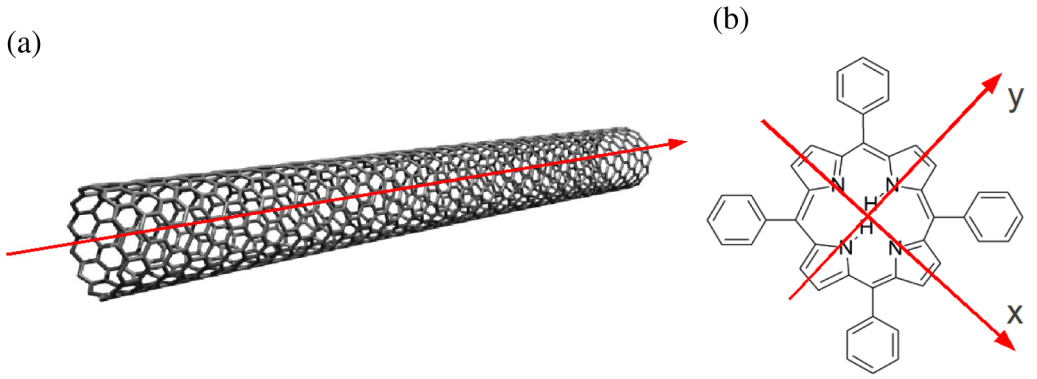

Figure 1. Scheme of (a) a single-wall carbon nanotube showing its axis, along which preferential light absorption and emission occur, (b) the H_2TPP molecule with its *x*- and *y*-axes, along which the optical oscillator strengths are almost identical. In the visible, the absorption is negligible for an incident polarization perpendicular to the plane of the molecule.[8]

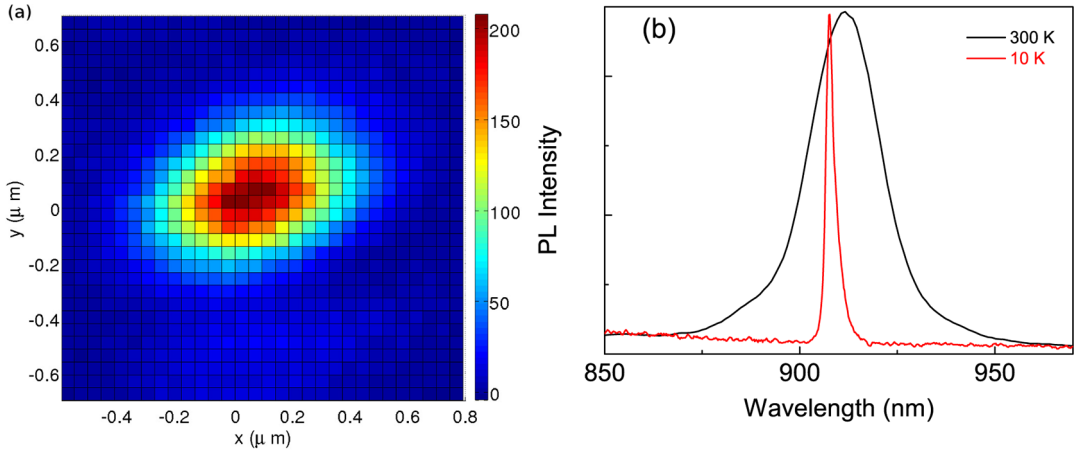

Figure 2. (a) Spatial map of the photoluminescence signal of a single nanocompound based on a (6,4) nanotube at room temperature. Detection wavelength: 912 nm, excitation wavelength 632.8 nm, incident power 100 W/cm^2. Color scale is in counts/s. (b) Normalized PL spectra of single (6,4) nanotubes at room temperature and low temperature. The broad (32 meV) PL at 300 K shrinks into one single narrow (3 meV) line at 10 K, which shows that the signal arises from a single nanotube.

extend over several nanometers outside of the nanotubes and lead to a strongly anisotropic energy transfer resonance despite the almost isotropic absorption of the chromophore. A simple model based on the electromagnetic response of a dielectric cylinder allows to account quantitatively for the excitation diagrams and to gain more insight into the local field map surrounding the nanotube.

Free base tetraphenyl porphyrin molecules (H_2TPP, see Figure 1b for the molecule structure) are noncovalently attached (Π-stacking) to the wall of carbon nanotubes (CoMoCat produced by Southwest Nanotechnologies SG65) by means of the micelle swelling method that we developed to achieve high-yield functionalization in water.[5] In solution, the average coverage of the nanotube wall by porphyrin molecules is on the order of 1 (one layer of porphyrins stacked on the nanotube wall with an almost 100% surface coverage).[5,6] In this type of sample, we showed by absorption and photoluminescence (PL) spectroscopies that an efficient energy transfer occurs, which leads to near-infrared luminescence of the nanotubes upon excitation of the Soret band of the porphyrin (440 nm).[5,7] Such an energy transfer has characteristic signatures in photoluminescence excitation (PLE) measurements. In this paper, we extend this technique to single nanocompound measurements, which allows us to reveal new anisotropic effects in the energy transfer.

Figure 2a shows the PL map of a 1.5 × 1.5 μm^2 area of the sample where the emission of a single nanocompound is visible. Figure 2b shows typical PL spectra of single nanocompounds at room and low temperature. The PL emission shrinks into a single narrow line (3 meV) at low temperature, clearly showing the presence of a single nanotube. The excitation spectrum of such nanocompounds (see next section) allows assigning their chiral family following the scheme introduced in ref 9. We need however to take into account the global red-shift of the transitions induced by the interaction with the H_2TPP molecules, as discussed in ref 5.

RESULTS AND DISCUSSION

Energy Transfer. In order to investigate energy transfer in individualized compounds, we performed

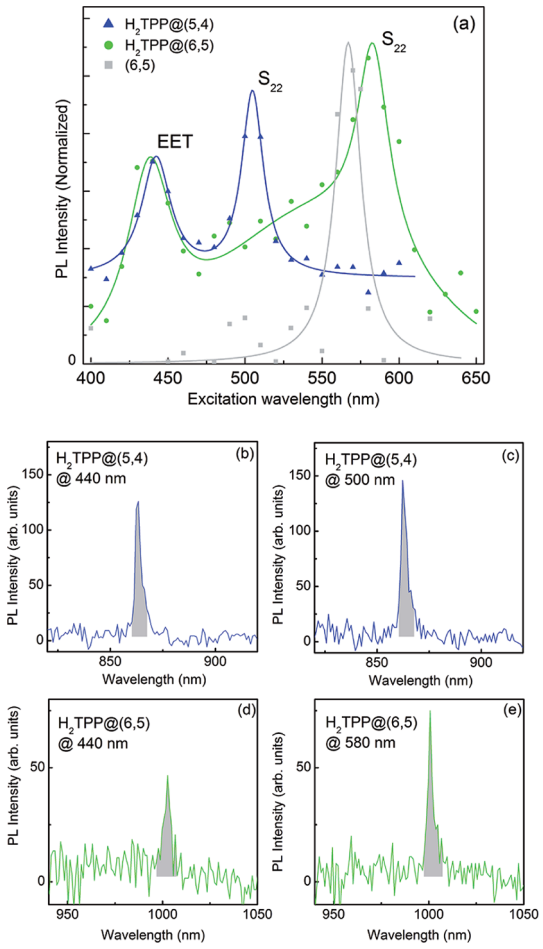

Figure 3. (a) Integrated photoluminescence intensity as a function of the excitation wavelength for two single nanocompounds based on a (5,4) nanotube (blue line, detection at 864 nm) and a (6,5) nanotube (green line, detection at 1002 nm). The gray line shows the spectrum of a bare (6,5) nanotube. (c and e) PL spectra of these nanocompounds excited at their S_{22} transition. (b and d) PL spectra of the same nanocompounds excited at the energy transfer resonance at 440 nm. All the spectra were divided by the excitation power and recorded at 10 K.

excitation photoluminescence spectroscopy on single nanocompounds by recording the NIR PL intensity of the nanotube while tuning the excitation wavelength. The NIR PL spectrum of each nanocompound consists of one narrow line whatever the excitation wavelength (see Figure 3b−e). The PLE spectrum is the integrated PL line intensity as a function of the excitation wavelength. Two typical results are shown in Figure 3a. The PLE spectra show two resonances for each compound. One of the resonances occurs at a wavelength that depends on the nanotube under investigation, whereas the other always appears at 440 nm. We assign the former to a direct excitation of the nanotube S_{22} excitonic transition, whereas the latter corresponds to a resonant excitation of the H_2TPP Soret band followed by energy transfer to the nanotube and NIR luminescence at the nanotube S_{11} excitonic resonance.

We first discuss the new insight given by such PLE measurements at the single nanocompound scale on the intrinsic properties of the nanotubes. The S_{22} resonances' widths are on the order of 60 meV, even at low temperature, which is very similar to the width obtained in ensemble measurements. This is in strong contrast with the lower S_{11} transition, which shows a line width on the order of 45 meV in ensembles but shrinks down to a few meV at the single-nanotube scale at low temperature. This means that inhomogeneous broadening is dominant for the lower transition but not significant for upper transitions. This is consistent with the reduced lifetime and dephasing time reported for these upper levels.[10−12] Importantly, we note that the functionalization of the nanotubes by the H_2TPP molecules does not induce any sizable broadening of the S_{11} transition, which remains on the order of a few meV at 10 K (see Figure 3b−e). This confirms that noncovalent functionalization hardly perturbs the electronic system of the nanotubes and preserves the phase coherence, although the latter is known to be very sensitive to environmental effects.

The second resonance showing up at 440 nm in all individual nanocompounds (and absent in bare nanotubes) corresponds to the observation of energy transfer at the single-nanocompound scale. Figure 3a shows a clear energy transfer resonance for both (5,4) and (6,5) nanotubes. Other results (not shown here) suggest that this energy transfer occurs whatever the chiral species, at least for the small-diameter nanotubes (up to a diameter of 1 nm) investigated in this study. An important point here is that the energy transfer yield, which is closely related to the ratio between the intrinsic resonance and the energy transfer resonance,[7] turns out to be constant (within a 20% error bar) when decreasing the temperature down to 10 K. This is consistent with previous time-resolved studies that showed an ultrafast process (on the order of 100 fs), in agreement with a pure electronic process (Dexter-type mechanism)[7,13] involving the overlap of the π orbitals of the chromophore and of the nanotube and leading to a very efficient energy transfer yield.[7]

Transfer Anisotropy. SWNTs are well known for their highly anisotropic optical properties, with light absorption and emission occurring essentially with a polarization parallel to the tube axis. In contrast, H_2TPP molecules absorb and emit light with an almost identical probability for polarizations along their *x*- and *y*-axes[8] (Figure 1b). No transition is expected for light polarized along the out-of-plane (*z*) axis. It is therefore interesting to check whether this in-plane isotropic absorption of H_2TPP can be used to modify the effective absorption properties of functionalized nanotubes and enhance their cross-polarized absorption through energy transfer.

Polarization spectroscopy is the perfect tool to address this issue. Although such a spectroscopy can

be performed in ensembles of randomly oriented objects,[14,15] it still suffers from *ad-hoc* instrumental corrections. In contrast, single-object spectroscopy allowed us to perform a thorough analysis of polarization effects in the optical properties of functionalized nanotubes. We investigated the role of the polarization of light in energy transfer processes where the donor has an isotropic absorption and where the acceptor is highly anisotropic.

We first checked the intrinsic properties of the nanotubes by analyzing the polarization diagram of the emitted light (S_{11} transition) and the absorption polarization diagram of the S_{22} transition by means of PLE measurements (Figure 4). We fit the data according to

$$I(\theta) = A\cos^2(\theta - \theta_0) + B\sin^2(\theta - \theta_0) \qquad (1)$$

where θ_0 stands for the nanotube axis direction in the sample plane and θ is the direction of the polarization of light (see inset of Figure 6). The results shown in Figure 4 are consistent with the literature: the dipole of the nanotubes is essentially along the tube axis.[10,16] We note that the extinction ratio, defined as B/A, is stronger in emission (~0.05) than in absorption (~0.15). This may be related to residual absorption from cross-polarized states or to the fact that the nanotube is not straight. In the latter case, the absorption has a perpendicular component, whereas emission can remain highly polarized since it arises from localized excitons.[17]

The polarization diagram of the energy transfer resonance is shown in Figure 5a for a (6,5)-based compound. Even if the absorption of light is expected to be quite isotropic for the H_2TPP molecules, the energy transfer resonance is clearly anisotropic, with a preferential axis identical to that of the S_{22} resonance (Figure 5b), which is the tube axis. Furthermore, the extinction ratio is on the order of 0.12, which is comparable to that observed for the S_{22} transition.

It is well known that the so-called crossed optical transitions (S_{12} for instance), which are allowed for an incident electric field perpendicular to the tube axis, are strongly suppressed in bare carbon nanotubes because of screening effects.[18] This can be understood as a consequence of the depolarizing field induced in the nanotube in response to an incident field, which

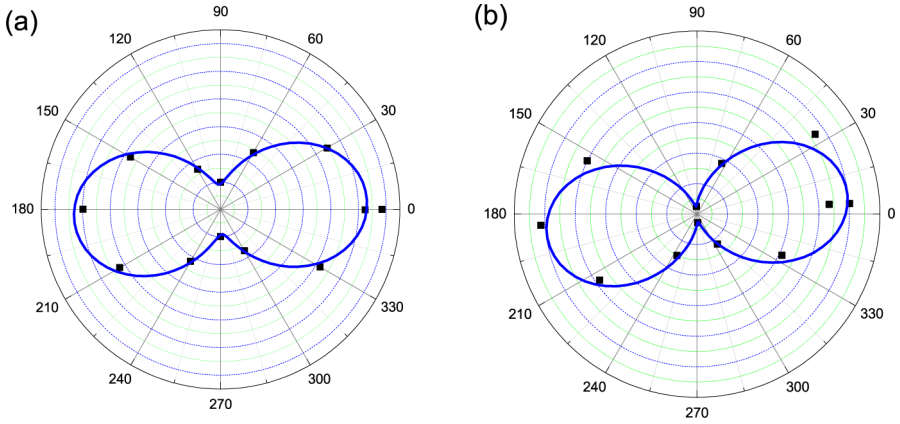

Figure 4. Polarization diagrams of a single NT/H_2TPP nanocompound based on a (6,4) nanotube. (a) Excitation diagram at 632.8 nm at the S_{22} transition. (b) Emission diagram (S_{11} transition at 912 nm). The blue solid line is a fit to the data according to eq 1. The axes of both diagrams are identical within an error bar of 10 degrees.

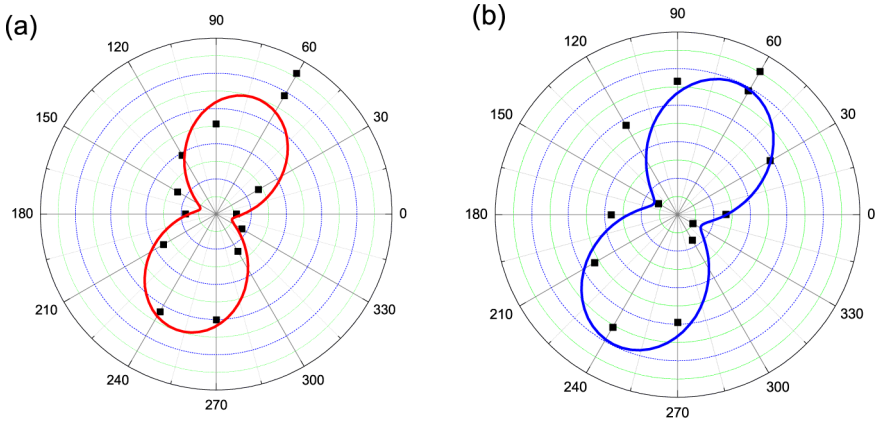

Figure 5. Polarization diagrams of a single nanocompound based on a (6,5) nanotube (same as in Figure 3). (a) Excitation diagram of the Soret transition at 440 nm (energy transfer). The red solid line is a fit to the data according to the local field model (see text) with $\varepsilon = 7$ and $\varepsilon_m = 2$. (b) Excitation diagram of the S_{22} transition at 580 nm. The blue solid line is a fit to the data according to eq 1.

causes a strong cancellation of the latter inside the nanotube. Similar local field effects occur at the surface of the nanotube and in its close vicinity. Therefore, we base our interpretation of the induced anisotropy in the energy transfer resonance on local field effects due to the large polarizability of the nanotube. This effect can be quantitatively accounted for by modeling the response of a dielectric cylinder (dielectric permittivity ε) of diameter d in a dielectric environment (dielectric permittivity ε_m) to an incoming field $\vec{E}_0$ and writing down the boundary conditions at the nanotube interface in the electrostatic approximation (valid for $d \ll \lambda$) (Figure 6).

For an incoming field $\vec{E}_0$ in the direction θ with respect to the tube axis (Oz) and in the limit of an infinite cylinder, the effective electric field at a point of cylindrical coordinates $M(r,\Phi,z)$ in the outer vicinity of the nanotube reads (Figure 6)

$$E_z^{\parallel} = E_0 \cos\theta \qquad (2)$$

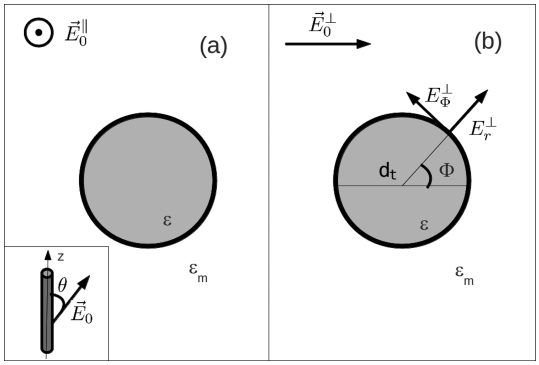

Figure 6. Response of a dielectric cylinder to an external electric field. Inset: Incoming field orientation with respect to the tube axis. (a) Parallel component. (b) Perpendicular component.

for the field component parallel to the tube axis, and

$$E_r^{\perp} = E_0 \sin\theta \left[1 - \frac{d^2}{4r^2}\frac{\varepsilon_m - \varepsilon}{\varepsilon_m + \varepsilon}\right]\cos\Phi \qquad (3)$$

$$E_\Phi^{\perp} = -E_0 \sin\theta \left[1 + \frac{d^2}{4r^2}\frac{\varepsilon_m - \varepsilon}{\varepsilon_m + \varepsilon}\right]\sin\Phi \qquad (4)$$

for the field components perpendicular to the tube axis.

An accurate value of ε of the nanotubes in the optical range is not available, but realistic values can be taken from calculations in the literature and turn out to be on the order of 5 to 30 for nonresonant and resonant conditions, respectively.[18,19] Therefore, the electric field can be strongly suppressed in a perpendicular geometry, whereas neither screening nor amplification is expected in the longitudinal geometry. The results of this simple model accounting for local field effects are summarized in Figure 7. In the close vicinity of the tube ($r - d/2 \ll d$), the field remains almost radial except for $\Phi \simeq \pm\pi/2$, where it becomes tangential with an amplitude reduced by a factor $(\varepsilon + \varepsilon_m)/2\varepsilon_m$. Bearing in mind that porphyrin absorption is forbidden for an electric field perpendicular to its plane, we can readily conclude that the absorption on the Soret band will be strongly suppressed for the perpendicular component (Figure 7b). In fact, although the local field amplitude can reach up to twice the amplitude of the incoming field, its direction remains essentially radial, that is, perpendicular to the average plane of the porphyrin molecule. On the other hand, for $\Phi \approx \pm\pi/2$, the field becomes parallel to the porphyrin plane, but its amplitude is strongly reduced. In total, the absorption of the porphyrin is strongly suppressed whatever its location on the tube surface. In contrast, its absorption is optimal for an incoming

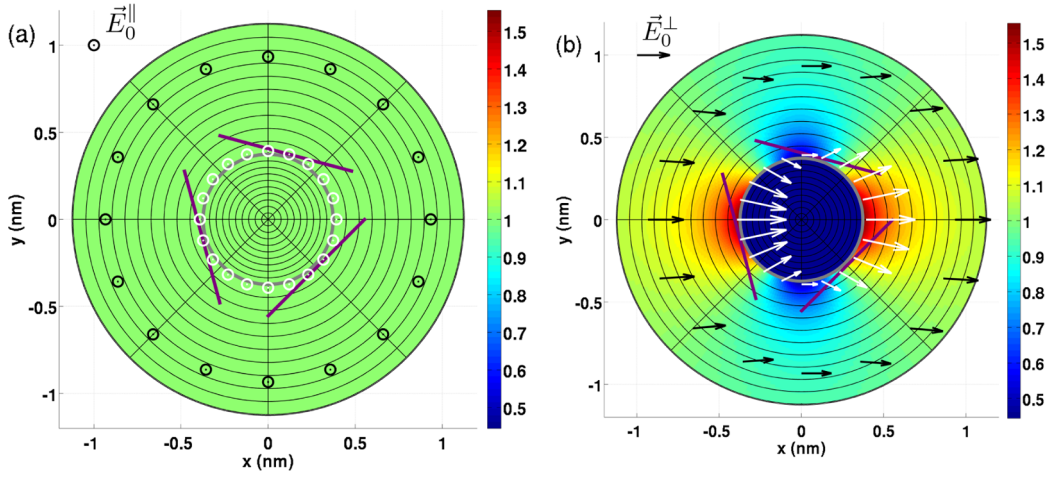

Figure 7. Local electric field amplitude in the vicinity of a nanotube for an incoming field parallel to the tube axis (a) or perpendicular to the tube axis (b) calculated from the model presented in the body of the paper. The arrows represent the electric field (amplitude and direction) on the outer tube surface (1.05 $d/2$, white arrows) and for a distance of 2.5 $d/2$ (black arrows). The field amplitude is in units of the incident field E_0. The porphyrin molecules are shown at a realistic scale on the surface of the tube (purple bars).

field parallel to the tube axis (Figure 6a and Figure 7a). As a consequence, the energy transfer resonance shows a strong anisotropy along the tube axis, whereas each individual chromophore has no preferential axis.

The first piece of information that arises from these experimental data is a clear confirmation of the local structural properties of the compound. Actually, this polarization effect can occur only if the H_2TPP molecules are properly attached with their plane stuck onto the nanotube wall. This would not be the case if the molecules were attached in an amorphous way or as small aggregates. Therefore, these polarization measurements first give an important insight into the molecular arrangement in the compounds, which was only predicted from energetic arguments before.

This anisotropy effect does not depend on the particular location of the porphyrin molecules on the nanotube wall (Figure 7). Actually, for a 500 nm long nanotube, several hundreds of porphyrin molecules are randomly attached on the wall, leading to a strong averaging even at the scale of a single nanocompound. Therefore, the right parameter for estimating quantitatively the anisotropy of the system is the average value $\langle|E_\Phi^\perp/E_0|^2\rangle_\Phi$ over all orientations ($E_r^\perp$ gives no contribution to the absorption since the absorption of H_2TPP is negligible for a field perpendicular to its plane). Actually, for $\theta = \pi/2$, $\langle|E_\Phi^\perp/E_0|^2\rangle_\Phi$ is directly comparable to the anisotropy coefficient B/A of the phenomenological fit (eq 1). The best fit to the data according to eq 4 is obtained for $\varepsilon = 7$, with $\varepsilon_m = 2$ (see Figure 5). The latter corresponds to a typical value for a transparent material such as the environment of the nanotubes. The value obtained for ε is in reasonable agreement with the values predicted for carbon nanotubes in the case of nonresonant frequencies.[18,19]

It is enlightening to use the ratio B/A to single out the role of the local field in contrast to a pure geometrical effect. In the latter case, $B/A = \langle\sin^2\ \Phi\rangle$ turns out to be 1/2, whereas the full local field model leads to $B/A \approx 0.1$, in much better agreement with the experimental value (on the order of 0.1 as well). This shows that local field effects due to the large polarizability of the nanotube are actually the main reason for the overall optical anisotropy of the compounds.

This study shows that local field corrections (or antenna effects) are essential in understanding the optical properties of nanocomposites. In particular, in the case of nanotubes, the large polarizability at optical frequencies allows to reshape drastically the absorption of the chromophore. The compounds inherit the spectral absorption features of the chromophore and the polarization absorption features of the nanotube. Although no significant local field amplification is observed in the particular case of semiconducting nanotubes (positive dielectric susceptibility), the effective absorption cross section of carbon nanotubes is clearly enhanced (by a factor of 5) due to the large number of attached chromophores and their large intrinsic absorption cross section. This opens the way to labeling applications where all semiconducting species could be excited efficiently with one single wavelength. In addition, new effects are expected for metallic nanotubes for which the negative dielectric permittivity can lead to strong local amplification of the electric field through surface plasmon resonances. In the latter case, the effective absorption (or scattering) of attached chromophores could be strongly enlarged, which is another attractive possibility in labeling or medical applications.[20]

CONCLUSION

We have investigated energy transfer in noncovalently bound porphyrin/carbon nanotube compounds at the single nanocompound level. Photoluminescence excitation spectroscopy reveals an efficient energy transfer from the porphyrin to the nanotube down to cryogenic temperatures, in line with a purely electronic process. Emission and excitation polarization diagrams allow to address the question of local field effects in the overall optical response of the nanocompound. We show that the compound inherits the spectral absorption features of the porphyrin together with the anisotropy of the nanotube, resulting in a strongly anisotropic energy transfer resonance. This result is quantitatively modeled by the electromagnetic response of a dielectric cylinder, which strongly modifies the field structure at the tube interface. This study opens the way to applications where nanotubes could serve as optical antenna especially in the case of metallic nanotubes that could benefit from an enhancement of the local field due to surface plasmon resonances.

METHODS

Material. The preparation of the micellar suspension of functionalized nanotubes is described in ref 5.

Micro-PL Setup. In order to investigate the energy transfer mechanism at the single-nanocompound scale, we deposit a drop of the suspension on the back side of a zirconium oxide hemispherical lens (solid immersion lens). Atomic force microscopy imaging shows that we reach a nanotube density on the order of 10 nanotubes per square micrometer with an average length of the nanotubes on the order of 500 nm. However, most of these nanotubes are not detected in our setup because we can only detect the semiconducting ones with a band gap in the detecting range of our CCD camera. Therefore, only the (5,4), (6,4), (8,3), (9,1), (6,5), and (7,5) chiral species are observed. This leads to an effective detectable tube density on the order of 10^{-1} μm^{-2}.[21] The solid immersion lens (SIL) configuration allows a strong enhancement of the signal due to an increase of the effective numerical aperture[22] and due to the reshaping

of the emission diagram of the emitter in the collecting direction. In contrast to a regular oil immersion objective, the SIL configuration is further compatible with low-temperature (10 K) measurements. The optical setup is based on a homemade confocal microscope. The light source is a high-brightness CW Xe lamp filtered by a monochromator and injected in a small-core optical fiber, or a He−Ne laser (632.8 nm). The excitation power ranges from 10 to 1000 W/cm^2. The injected and collected beams are polarized and analyzed by a rotating achromatic half-wave plate associated with a polarizer with a fixed direction. The collected light is dispersed in a 32 cm spectrometer and detected by a nitrogen-cooled Si CCD camera.

PLE Measurements. PLE spectra are obtained by recording a full PL spectrum for each excitation wavelength. Then, for each PL spectrum, the PL line of the nanotube is extracted, integrated over its width, and divided by the incident excitation power. This normalized PL intensity is reported as the PLE intensity for each excitation wavelength.

Conflict of Interest: The authors declare no competing financial interest.

Acknowledgment. C.R. and F.V. contributed equally to this work. C.V. is a member of "Institut Universitaire de France". The authors are thankful to G. Clavier and T. Heinz for helpful discussions. This work was partly funded by the grants ANR TRANCHANT and C'Nano IdF TENAPO.

REFERENCES AND NOTES

1. Avouris, P.; Freitag, M.; Perebeinos, V. Carbon Nanotube Photonics and Optoelectronics. *Nat. Photonics* **2008**, *2*, 341–350.
2. Sgobba, V.; Guldi, D. M. Carbon Nanotubes Electronic/Electrochemical Properties and Application. *Chem. Soc. Rev.* **2009**, *38*, 165–184.
3. Ehli, C.; Oelsner, C.; Guldi, D. M.; Mateo-Alonso, A.; Prato, M.; Schmidt, C.; Backes, C.; Hauke, F.; Hirsch, A. Manipulating Single-Wall Carbon Nanotubes by Chemical Doping and Charge Transfer with Perylene Dyes. *Nat. Chem.* **2009**, *1*, 243–249.
4. Borghetti, J.; Derycke, V.; Lenfant, S.; Chenevier, P.; Filoramo, A.; Goffman, M.; Vuillaume, D.; Bourgoin, J.-P. Optoelectronic Switch and Memory Devices Based on Polymer-Functionalized Carbon Nanotube Transistors. *Adv. Mater.* **2006**, *18*, 2535–2540.
5. Roquelet, C.; Lauret, J.-S.; Alain-Rizzo, V.; Voisin, C.; Fleurier, R.; Delarue, M.; Garrot, D.; Loiseau, A.; Roussignol, P.; Delaire, J. A.; *et al.* Pi-Stacking Functionalization of Carbon Nanotubes through Micelle Swelling. *ChemPhysChem* **2010**, *11*, 1667–1672.
6. Roquelet, C.; Garrot, D.; Lauret, J. S.; Voisin, C.; Alain-Rizzo, V.; Roussignol, P.; Delaire, J. A.; Deleporte, E. Light Harvesting with Noncovalent Carbon Nanotubes/Porphyrin Compounds. *Chem. Phys.* **2012**, DOI: 10.1016/j.chemphys.2012.09.004.
7. Roquelet, C.; Garrot, D.; Lauret, J. S.; Voisin, C.; Alain-Rizzo, V.; Roussignol, P.; Delaire, J. A.; Deleporte, E. Quantum Efficiency of Energy Transfer in Noncovalent Carbon Nanotube/Porphyrin Compounds. *Appl. Phys. Lett.* **2010**, *97*, 141918–3.
8. Palummo, M.; Hogan, C.; Sottile, F.; Bagala, P.; Rubio, A. *Ab Initio* Electronic and Optical Spectra of Free-Base Porphyrins: The Role of Electronic Correlation. *J. Chem. Phys.* **2009**, *131*, 084102–7.
9. Bachilo, S. M.; Strano, M. S.; Kittrell, C.; Hauge, R. H.; Smalley, R. E.; Weisman, R. B. Structure-Assigned Optical Spectra of Single-Walled Carbon Nanotubes. *Science* **2002**, *298*, 2361–2366.
10. Lefebvre, J.; Finnie, P. Polarized Photoluminescence Excitation Spectroscopy of Single-Walled Carbon Nanotubes. *Phys. Rev. Lett.* **2007**, *98*, 167406–4.
11. Lauret, J. S.; Voisin, C.; Cassabois, G.; Delalande, C.; Roussignol, P.; Jost, O.; Capes, L. Ultrafast Carrier Dynamics in Single-Wall Carbon Nanotubes. *Phys. Rev. Lett.* **2003**, *90*, 057404–4.
12. Manzoni, C.; Gambetta, A.; Menna, E.; Meneghetti, M.; Lanzani, G.; Cerullo, G. Intersubband Exciton Relaxation Dynamics in Single-Walled Carbon Nanotubes. *Phys. Rev. Lett.* **2005**, *94*, 207401–4.
13. Garrot, D.; Langlois, B.; Roquelet, C.; Michel, T.; Roussignol, P.; Delalande, C.; Deleporte, E.; Lauret, J.-S.; Voisin, C. Time-Resolved Investigation of Excitation Energy Transfer in Carbon Nanotube-Porphyrin Compounds. *J. Phys. Chem. C* **2011**, *115*, 23283–23292.
14. Lakowicz, J. R. *Principles of Fluorescence Spectroscopy*; Plenum Press: New York, 1983.
15. Miyauchi, Y.; Oba, M.; Maruyama, S. Cross-Polarized Optical Absorption of Single-Walled Nanotubes by Polarized Photoluminescence Excitation Spectroscopy. *Phys. Rev. B* **2006**, *74*, 205440–6.
16. Reich, S.; Thomsen, C.; Maultzsch, J. *Carbon Nanotubes: Basic Concepts and Physical Properties*; Wiley-VCH: Weinheim; Cambridge, 2004.
17. Galland, C.; Högele, A.; Türeci, H. E.; Imamoğlu, A. m. c. Non-Markovian Decoherence of Localized Nanotube Excitons by Acoustic Phonons. *Phys. Rev. Lett.* **2008**, *101*, 067402–4.
18. Uryu, S.; Ando, T. Exciton Absorption of Perpendicularly Polarized Light in Carbon Nanotubes. *Phys. Rev. B* **2006**, *74*, 155411–9.
19. Wan, X.; Dong, J.; Xing, D. Y. Optical Properties of Carbon Nanotubes. *Phys. Rev. B* **1998**, *58*, 6756–6759.
20. Cheng, H.; Zhao, Y.; Fan, Y.; Xie, X.; Qu, L.; Shi, G. Graphene-Quantum-Dot Assembled Nanotubes: A New Platform for Efficient Raman Enhancement. *ACS Nano* **2012**, *6*, 2237–2244.
21. Berciaud, S.; Cognet, L.; Poulin, P.; Weisman, R. B.; Lounis, B. Absorption Spectroscopy of Individual Single-Walled Carbon Nanotubes. *Nano Lett.* **2007**, *7*, 1203–1207.
22. Moehl, S.; Zhao, H.; Don, B. D.; Wachter, S.; Kalt, H. Solid Immersion Lens-Enhanced Nano-Photoluminescence: Principle and Applications. *J. Appl. Phys.* **2003**, *93*, 6265–6272.